Environmental Modelling and Software 134 (2020) 104868

Contents lists available at ScienceDirect

Environmental Modelling and Software

journal homepage: http://www.elsevier.com/locate/envsoft

Integrated remote sensing and GIS approach using Fuzzy-AHP to delineate and identify groundwater potential zones in semi-arid Shanxi Province, China

Zhenfeng Shao [a,1], Md. Enamul Huq [a,1,*], Bowen Cai [a], Orhan Altan [b], Yan Li [c]

[a] State Key Laboratory of Information Engineering in Surveying, Mapping and Remote Sensing, Wuhan University, 129 Luoyu Road, Wuhan, 430079, Hubei, China
[b] Istanbul Technical University, Department of Geomatics, Istanbul, 36626, Turkey
[c] Inner Mongolia Electronic Information Vocational Technical College, No. 8, Suergan Street, Saihan District, Hohhot, Inner Mongolia, China

ARTICLE INFO

Keywords:
Remote sensing
GIS
Fuzzy-AHP
Groundwater
Northern China

ABSTRACT

In Shanxi Province, China, groundwater is a major problem and exploration of groundwater potential zones (GWPZs) is a great necessity. This paper contributed to integrate RS-GIS to delineate GWPZ and applied Fuzzy-AHP method in a single platform. The main objective includes delineation GWPZs with RS and geo-environmental factors using Fuzzy-AHP method. Fuzzy-AHP method was employed to calculate weight of factors. RS-GIS was used to create maps and discover groundwater availability. GWPZs were classified in five separate classes. Results indicated that 13.26%, 27.02%, 26.35%, 23.64%, and 9.71% area classified as very good, good, moderate, poor, and very poor GWPZs. The validated analytical results revealed 82.5%, 12.3%, 3.5%, and 1.7% existing water wells exhibited in very good, good, moderate, and poor/very poor GWPZs. This indicates Fuzzy-AHP model generated findings were in very good agreement with ground-truth data. This RS-GIS based Fuzzy-AHP method is proficient and efficient in identification and delineation of GWPZs.

1. Background

1.1. Introduction

Groundwater is a key resource of natural water and varies geographically and temporally. It plays an important role in preserving the ecological balance, environmental stability, human well-being, and economic development (Arefin, 2020; IPCC, 2001). Owing to the growing population, enlarged irrigated cultivated area, and economic development, the use of and demand for groundwater has increased continuously with very little or no consideration of the importance of groundwater environmental balance (Nhamo et al., 2020; Zhang et al., 2019). Globally, approximately 36%, 42%, and 27% of the overall groundwater extraction are used for household, agricultural, and industrial purposes, respectively (Patra et al., 2018). Groundwater is one of the key sources of water for arid/semi-arid areas of northern China, as in. It is also used by 70% of the population for drinking, and in the dry regions in China including Shanxi Province, over 40% of the available groundwater is used to irrigate farmland (Yin et al., 2018). In addition, owing to increasing socio-economic growth, groundwater demand in this region has also increased in recent years. Regretfully, the shortage of groundwater has created a threat to the local inhabitants of this province (Huq et al., 2018a; Zhu et al., 2017). Therefore, the identification and assessment of critical parameters are necessary for predicting groundwater potential (Patra et al., 2018). In addition, demand for freshwater has increased worldwide since the last century because of industrial expansion and rapid population growth (Arefin, 2020; Zhang et al., 2019). GWPZ delineation is needed for sustainable groundwater usage. In China, Shanxi Province is situated in one of the driest areas, known as a water shortage area (Zhu et al., 2017). Therefore, identifying the presence of groundwater is the most important issue for authorities. Ordinary groundwater identification and delineation techniques include drilling, geological, hydrogeological, and geophysical methods as well as field surveys. This requires extensive labor for activities such as exploration, which is costly in terms of time, money, and resources, and requires the participation of experts (Achu et al., 2020; Arefin, 2020; M. M. et al., 2020; Nhamo et al., 2020; Shao et al., 2019a). However, the use of modern technologies, such as Geographic Information Systems (GIS)

* Corresponding author.
E-mail addresses: enamul_huq@whu.edu.cn, polton86@gmail.com (Md.E. Huq).
[1] These authors contributed equally to this work.

https://doi.org/10.1016/j.envsoft.2020.104868
Accepted 3 September 2020
Available online 9 September 2020

and remote sensing (RS), is less expensive, more responsive, and more convenient.

The incorporation of RS and GIS is a paradigm shift for groundwater research, which supports the evaluation, monitoring, and preservation of groundwater resources (Silwal and Pathak, 2018). These tools can be useful in the exploration of groundwater mapping. Furthermore, RS, apart from its usefulness in the selection of potential areas of groundwater exploration, also provides inputs for estimating groundwater resources. Integrating RS and GIS into the mapping of groundwater potentiality enables the storage, manipulation, and analysis of data in different forms and magnitudes (Abijith et al., 2020; Ahmad et al., 2020; Shao and Cai, 2018; Shao et al., 2018; Siddi Raju et al., 2019; Yin et al., 2018). These data layers exhibit a common coordinate system, which can be exploited to create thematic maps within the entire study area (Oikonomidis et al., 2015). Several estimation methods have been employed to evaluate a GWPZ, such as multifactor analysis (Chen et al., 2010), single-factor analysis (Xin-feng et al., 2012), fuzzy clustering (Ahmad et al., 2020), GIS information fusion (Siddi Raju et al., 2019), brittle rock proportion (Singaraja et al., 2015), and Fuzzy-AHP indices (Pinto et al., 2017). In the current study, the analytic hierarchy process (AHP) (Saaty, 1990), Fuzzy model (Zadeh, 1965), and RS-GIS methods are used to delineate GWPZ. In addition, seven factors including geomorphology, slope, NDVI, drainage density, rainfall, LULC, and soil type were used to identify the GWPZs. AHP is a strong decision-making method with various factors (Mohammadi-Behzad et al., 2018; Pinto et al., 2017). The combination of GIS and AHP could be described as a mechanism for modifying and organizing geographical details and weight (Mumtaz et al., 2019). In traditional set theory, an object either fits or does not fit into a set; consequently, there is no partial membership, which prevents certain concepts with transitional membership from being modeled. The Multi criteria decision analysis (MCDA) is recognized as a significant tool to formalize and address the environmental challenges and decision making (Steele et al., 2009). The general objective of MCDA is for determining an option from several existing preferences. Different spatial challenges have raised for GIS-MCDA. The MCDA methods have been applied to some hydrological indicators to predict spatial potential areas for groundwater resources. For example, Adiat et al. (2012) explored the fitness of GIS-MCDA as a spatial estimate tool for groundwater potential zones in Kedah and Perlis states, Malaysia. They also examined the coherence effect of criteria on the effectiveness of MCDA as a prediction tool and introduced that GIS-MCDA method is efficient to produce proper and consistent prediction. However, Singh et al. (2017) evaluated rainwater harvesting potential and worthy locations of it and simulated recharge structures applying GIS-MCDA in Canal Command of Eastern India. Additionally, Murthy and Mamo (2009) identified GWPZs in Moyale-Teltele sub-basin, South Ethiopia using MCDA method. Moreover, Ajibade et al. (2019) delineated the suitable zones for solid waste disposal as well as management with integration of GIS and MCDA in Akure, Ondo State, Nigeria. However, Fuzzy set theory can solve this problem (Zadeh, 1965). This theory has been revised and improved by multiple researchers to simplify its use (Cagman et al., 2011; Liu and Pedrycz, 2009).

In Shanxi Province, China, there are numerous studies on groundwater that have been performed. For example, Zhang et al. (2012) applied step-by-step logistic regression with some environmental explanatory parameters and RS data to construct a 2D geospatial model that predicts the regions of high As risk potential in Shanxi Province. Zhang et al. (2013) also used a statistical model to forecast the high As risk area in this region. Results show that approximately 3000 km^2 of the province were at a high risk of As concentration above 50 mg L^{-1}. Additionally, the assessment of groundwater geochemistry was performed by Hu et al. (2013) and Tang et al. (2013) using geochemical processes to control fluoride mobility and iodine-rich groundwater in this region. Moreover, in a recent investigation (Huq et al., 2018a) in this region, found that the acceleration and release of As in the groundwater of Datong Basin in Shanxi Province are determined by the responsible controlling factors.

Much effort has been undertaken in the study of the groundwater system in Shanxi Province based on hydrology, geochemistry, and hydrogeochemistry. However, no investigations have been conducted to detect or delineate the potential groundwater zone in this province. Therefore, the aims of the study are the following: (1) to propose a methodology to identify and delineate different GWPZs based on several groundwater potential factors using integrated RS-GIS techniques with Fuzzy-AHP to ensure the conservation, sustainability, and management of groundwater resources in Shanxi Province, China; (2) to analyze the relationship between each contributing factor for groundwater; and (3) to conduct a model validation and sensitivity analysis to determine the most important factors influencing the detection of possible groundwater zones. The scientific contribution of this paper is integration of RS-GIS for GWPZ and combined application of Fuzzy-AHP method. In addition, it presents an analysis of GWPZ mapping with the integration of RS-GIS to develop a supplemental or modifying method for delineating groundwater. Moreover, the efficiency of GWPZ mapping was validated through the use of ground-truth data (existing wells in this region).

1.2. Applications of RS and GIS in groundwater mapping

The explanatory satellite data development since 1990s offers unexampled opportunities for supporting and improving water resource management. It is applied to understand sub-surface water environment (Todd and Mays, 1980). Using satellite data in groundwater problems might support to general scientific tendency toward a big-picture view for the groundwater issues. Toth (1963) hypothesized groundwater flow systems in various scales depending on topographic factors. Toth's topographically derived flow model proposed that RS may be much effective to predict groundwater flows, because it presents more scope to detect groundwater. Satellite-based sensors are presently capable to make direct as well as indirect measurements of almost all elements of hydrological cycle (Jasmin and Mallikarjuna, 2011). These sensors are thus able to provide critical data for supporting of water resources management.

Previously, satellite data could not be used for groundwater study, because groundwater is located inside the earth. Radar from the air and satellites, as well as radiometers, can typically penetrate only a few centimeters below the earth's surface (Jasmin and Mallikarjuna, 2011). Nevertheless, groundwater indicators obtained from remote sensing provide fundamental data; however, traditional substitutes are not accessible. Recently, satellite data have been used to retrieve groundwater head levels, fluctuations of groundwater concentration, heat characteristics, and subsidence data (Abijith et al., 2020; Ma et al., 2020). Satellite technology is analyzed in terms of its capacity to estimate groundwater potentiality, availability, and flow. Satellite data (Table 1), required if ancillary research is to be conducted, can be used to explore the behavior of groundwater from the surface. Furthermore, RS data are most advantageous when integrated with a quantitative model, GIS, and ground-truth data (Mohammadi-Behzad et al., 2018).

Integration of RS-GIS for groundwater is a paradigm shift in groundwater research that helps for assessing, observing, and conserving of groundwater resource. The set of RS-GIS tools are useful to research in groundwater resource management (Mahmoud and Alazba, 2016). In addition, these show a significant relationship in extensive groundwater resource study and management. Recent progresses of RS-GIS exhibit a vital tool to explore groundwater (Shao et al., 2019a). Satellite-based RS systems provide comprehensive, correct, unbiased, and readily accessible data regarding location, scope, as well as progressive of changes. The effective application of RS for lineaments has identified as powerful tool thought it is associated to faults and cracking in hard-rock (Jasmin and Mallikarjuna, 2011). However, RS-GIS technologies are efficient to handle and manage a large and multifaceted

Table 1
List of reactive space-based sensors that provide data for the investigation of groundwater potentiality (Carleer and Wolff, 2006; Crétaux et al., 2011; Gaber et al., 2010; Hall et al., 2008; Lavender and Groom, 1999; Song and Park, 2014; Turk and Miller, 2005).

Sensor	Launch year	Resolution (m)	Precipitation	Surface temperature	Soil moisture	Water storage	Snow water	Land cover	Topography
AMSR-E	2002	5400–56,000	●	●	●		●		
ASTER	1999	15,30,90		●				●	●
AVHRR	1991–2003	1100	●	●	●		●		
GRACE	2002	300,000				●			
ENVISAT-RA-2	2002	1000		●					●
Landsat-7	1999	30,60		●				●	
MODIS	1999	250,50,1000		●				●	
OrbView-2	1997	1100		●				●	
OrbView-3	2003	1,4		●				●	●
RADARSAT-1	1995	8–100			●				
SRTM	2000	30,90							●

database for groundwater research. The high-quality RS data and integration of corresponding thematic maps in a sophisticated GIS environment confirm and increase to predict groundwater potential location accurately (Achu et al., 2020).

The integration of RS and groundwater flow projections is an easy approach to identifying the boundary of a lake, river, reservoir, seepage area, or drainage or evapotranspiration zone. RS data are also suitable in the preparation of a respective thematic map(s), assignment of proper weights, and convergence in an advanced GIS environment. This guarantees and improves the accuracy of forecasting the location and groundwater capabilities of promising areas (Abijith et al., 2020; Shao et al., 2019b; Silwal and Pathak, 2018). The combination of RS and GIS is a vital data source for producing hydrogeological maps, including the use of RS in the management of water resources, hydrogeological

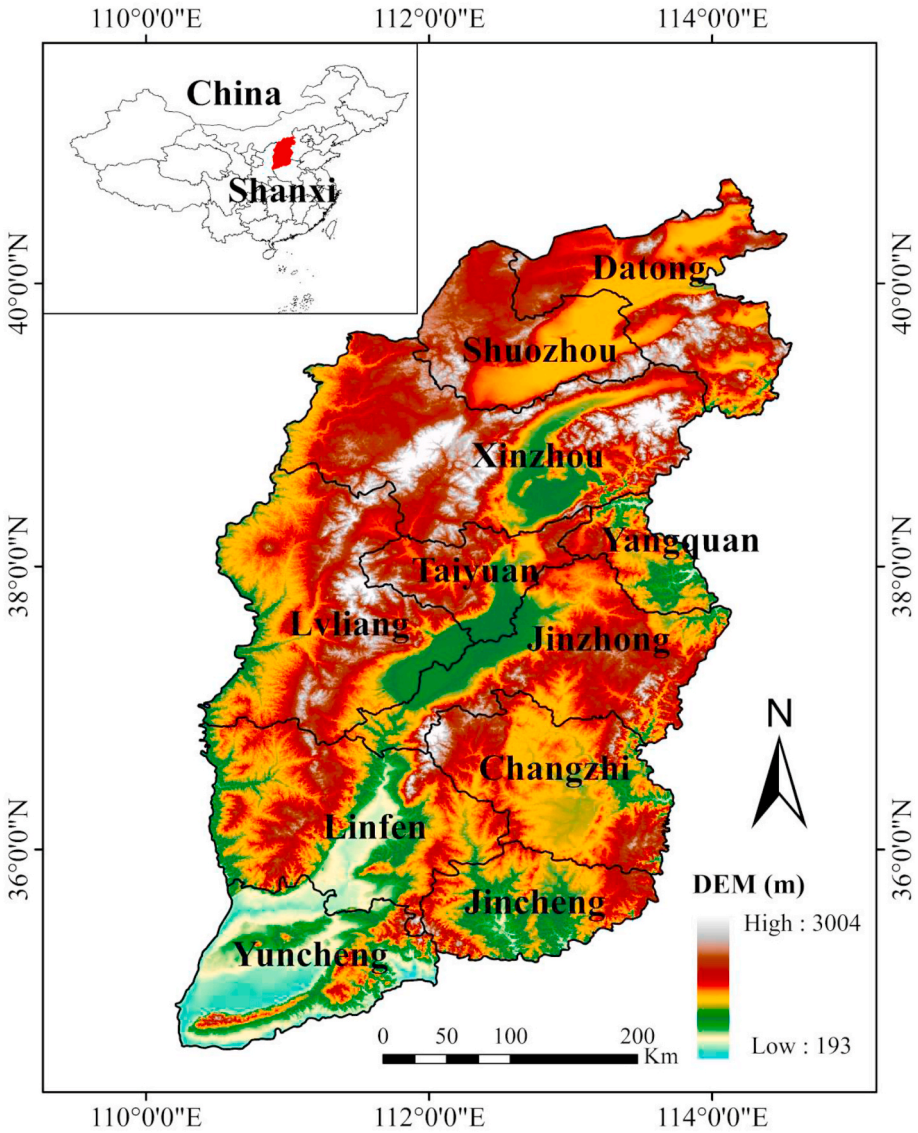

Fig. 1. The location and Digital Elevation Model (DEM) of Shanxi Province, China.

modeling, and mapping, the identification and tracking of salinization-impacted zones, biomass determination, land use and crop classification/selection, and environmental protection and monitoring (Achu et al., 2020; Arefin, 2020; Mahmoud and Alazba, 2016).

The nature of groundwater is progressive; therefore, the incorporation of RS data with GIS is very useful for identifying GWPZs (Mahmoud and Alazba, 2016). Satellite data offer fast and accurate guidelines as well as information on diversified factors that control groundwater occurrence and movement directly and/or indirectly (Jasmin and Mallikarjuna, 2011). Additionally, GIS provides an eminent work environment for the efficient handling of comprehensive and sophisticated spatial–temporal data (Patra et al., 2018). RS is a suitable tool for regions in which geological, hydrogeological, and field data are inadequate or missing (Yousif et al., 2018). Many existing studies (Mahmoud and Alazba, 2016; Mohammadi-Behzad et al., 2018; Oikonomidis et al., 2015; Pinto et al., 2017; Shao et al., 2019b; Siddi Raju et al., 2019; Yousif et al., 2018) have extensively employed RS with GIS techniques to assess the GWPZ.

2. Study area description

2.1. Location and climate

Shanxi Province in northern China is situated in the East Asian monsoon zone, characterized by an arid and semi-arid climate. Mountains, such as Heng Mountain, Zhu Mountain, Wutai Mountain, Zhoushan Mountain, Taihang Mountain, Taiyue Mountain, and Zhongtiao Mountain, constitute the boundaries of the entire province, and the topography slopes down from northwest to southeast (Fig. 1). It is situated between 34 34′ N and 40 44′ N latitude and 110 14′ E and 114 33′ E longitude and covers approximately 1,567,000 km^2 (Zhu et al., 2017). It also exhibits a typical semi-arid and arid climate. The average yearly rainfall is between 358 and 621 mm, the evaporation is approximately 1000 mm, and 60% of the annual precipitation occurs in July and August. The annual air temperature of the area is between 4.2 and 14.2 °C with an average temperature of 6.5 °C (Li et al., 2017; Su et al., 2016).

2.2. Geological features

The eastern, western, and northern parts of the study location contain bedrock outcrops. The bedrock predominantly originates from the Archean gneiss and the basalt of the Wutai Group of southern part, the Archean gneiss of the Sanggan family and Sinian limestone of the northern area, and the Cambrian-Ordovician limestone and Carboniferous-Permian-Jurassic sandstones and shale of the west. The gneiss and basalt of the Hengshan segment of the Archean are to the east. The Hengshan Mountains comprise primarily the Neoarchaean Hengshan complex, composed of migmatite, tonalite, granodiorite, and granite gneiss along with pegmatite, granite, and mafic lenses. The Lower Paleozoic, from both the Cambrian and Ordovician, containing deposits of limestone, is found in the Guancen Mountains.

The Honshu ranges belong to the Permian era and, hence, existed before the Cretaceous clastic rocks (Li et al., 2017). The Cretaceous clastic rocks include shale, sandstone, and coal. In the northern region of Shanxi, early-middle Pleistocene basalt and new Tertiary lateral soils were uncovered by the late-middle and early Tertiary Pleistocene basalt. The sediments from the Cenozoic era varied from shallow-deep in the range of 50–2500 m. Generally, grain size of sedimentary rock declines from the edge to the center. Sediments covering the middle part of the study region are a diverse series of lateral sandy loam soils, silts, discontinuous alluvial–pluvial sands, alluvial-lacustrine sandy loam layers, lacustrine soils, and natural-matter-enriched and silk clays (Zhu et al., 2017). Therefore, sediments in this region are typically favorable toward humic materials, such as plants and algae.

Analysis of mollusk fossils as well as micro-fossil (Ostracoda fossil) sculptures identified four main stratigraphic units (Fig. 2) of Quaternary sediments (Q1-Q4) in this area: (1) stratigraphic unit of Early Pliocene: developed in the static hydrodynamic environments from the extension of a paleo-lake, it comprises a sequence of sediments from soft clay to clay with a grayish and gray-green color. The depth of such a sedimentary chain is usually higher than 200 m; (2) before the Middle Pliocene stratigraphic unit: the sedimentary sequence varies from 20 to 30 m with a composition of grayish yellow silt as well as silty clay. The top section of this sequence is formed with fine-medium sand; (3) before the Middle Pleistocene stratigraphic unit: the sequence of this unit is distinguished by a gray and grayish yellow fine sand as well as a silty fine sand. The deposition setting is characterized by the interchange of the lakeside with the shallow lake, resulting in regular changes in the lake level and corresponding hydrodynamic state. Typically, the depth of this unit ranges between 30 and 50 m; (4) late Pleistocene to Holocene stratigraphic unit: lithologies include gray-green to greyish yellow fine sand, deep gray, clay, and silt. The deposition condition is affected with regular changes in the level of the lake and its hydrodynamic environment. The thickness of this unit is roughly 30 m.

2.3. Hydrological conditions

There are more than 1000 large and small rivers in the Shanxi Province, predominantly seasonal rivers, with a wide seasonal fluctuation in the water flow. There are five large rivers in this province covering more than 10,000 km^2, namely, the Fenhe and Qinhe rivers in the Yellow River Basin and the Sanggan, Zhanghe, and Hutuo rivers in the Haihe River Basin (Zhu et al., 2017). These rivers are the primary surface water source and system of this region. However, the upstream reservoir, which has developed as a primary source of irrigation for agriculture, has significantly changed the conditions of the rivers. Two types of regular and extensive irrigation operations are held in March and September every year. Soil salinization is recognized as an important problem in this area (Li et al., 2017). Studies of RS techniques have shown that nearly 25–30% of the entire basin is covered with saline soil. The aquifer materials of the Shanxi Province are composed mainly of alluvial–pluvial sand from the Middle to Late Pleistocene. Quaternary groundwater systems are usually found in lacustrine, alluvial-lacustrine, and alluvial-pluvial aquifers. The first group (depth between 5 and 50 m) is known as the upper group, whereas the middle aquifers are 5–150 m deep and the lower aquifers have depths greater than 150 m (Zhang et al., 2013). The runoff of non-perennial water from the river and the return flow of irrigation are the recharge sources for groundwater in this region. The entire Quaternary groundwater system shows a complex hydrogeological structure and can be characterized into three classes-unrestricted, semi-restricted, and restricted aquifers. Vertically infiltrating precipitous water, lateral penetrating groundwater at the front of the mountains, which usually originates from the bedrock, the leaking of river water, and irrigation runoff replenishes the upper aquifer, whereas discharge occurs mainly through evapotranspiration and artificial extraction. Deep aquifers are recharged by adjacent bedrock aquifers as well as top unrestricted and semi-restricted aquifers and are discharged mostly by artificial abstraction (Hu et al., 2013). Recharging the system of shallow aquifers is limited as a result of dry climatic conditions. This occurs particularly around the edges where the outcropping sediments are more porous, owing to the weak hydraulic gradient throughout the Shanxi region and the availability of fine-grained, poorly porous sediments in the low-lying center of the area. In this region, groundwater typically flows from the northwest to the southeast in the middle and from the front of the mountain to the central parts of the area. Groundwater flow is normally slow, and mainly occurs in the deep aquifers.

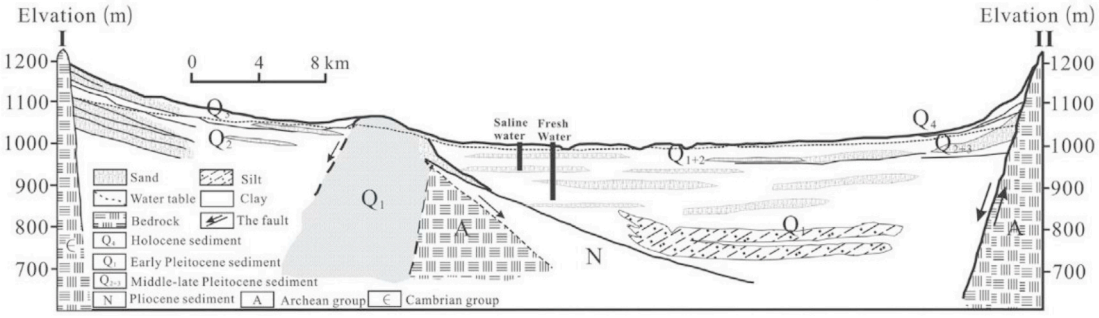

Fig. 2. Hydrogeological cross-section with transect line labeled of the study area (modified from (Guo and Wang, 2005)).

3. Materials and methods

3.1. Identifying factors influencing groundwater potentiality

Numerous causes affect the distribution and renewal of groundwater. The groundwater situation of any specific region can differ significantly owing to the different factors that affect the occurrence and recharge of groundwater (Huq et al., 2018b; Mahmoud and Alazba, 2016). These factors are usually measured at various scales and are represented in maps. Due to variance in scales, factor maps are created at equal scales for multifactor decision-making that categorizes the factor maps in suitable classes. The suitable classes then serve as the source for consistent mapmaking with all included factors. In the present study, seven factors were chosen for GWPZ mapping. The factors are presented in form of seven thematic layers, specifically, geomorphology, slope, rainfall, normalized difference vegetation index (NDVI), drainage density, land use/land cover (LULC) classification, and soil type. All these factors are interdependent and are considered as a single factor for classifying the GWPZ. To select the most important factors, four assumptions were made that are most influential in increasing the groundwater potentiality: (1) increasing groundwater recharge (rate of precipitation penetration), (2) high penetrability of soils and rocks (geological and lithological units), (3) higher drainage density, and (4) flat slopes.

3.2. RS satellite data to prepare groundwater potential zones

In this study, RS satellite data were employed to create thematic maps (layers) of several factors that influence groundwater potentiality over the study region. Groundwater recharge is a process in which water tables are recharged through the injection of water from an unsaturated zone to a saturated zone. Satellite data from the Shuttle Radar Topography Project are used to retrieve information regarding the slope and drainage density distribution in Shanxi Province. Structural components, typically slope and drainage density, play a significant role in the storage of groundwater, in which they serve as a conduit to groundwater. High drainage density zones are suitable for high surface runoff but not for infiltration. The gentle slope regions (<5°) are favorable for water infiltration. LULC is obtained from processed Landsat 8 satellite data. NDVI is prepared based on spot/vegetation and moderate resolution imaging spectroradiometry data. Geomorphology, soil, and rainfall data are extracted from the China geomorphology atlas, and China soil type and rainfall observation data, respectively. Afterwards, thematic layers were produced from the application of original factors to the RS dataset and GIS, as the dataset contained diverse features, such as spatial resolution, protection, and format. Therefore, all the datasets were transformed into guaranteed equal features, converted to a grid format, and re-projected with a WGS-84 system.

3.3. Determining factor weights

Multi-criteria decision-making (MCDM) is a key tool for water resources management that includes structure and rigor in the decision-making. An MCDM technique, such as the analytic hierarchy method (AHP), is a systematic and scientifically established method for studying qualitative measures. AHP provides a platform for comparing parameters in pairs at each layer in a hierarchy structure and can assess the comparative standard coefficient weights with alternative schemes. Additionally, Fuzzy logic generally offers an easy technique for drawing definite conclusions from uncertainty and inaccurate information (Balezentiene et al., 2013). Moreover, the AHP method of MCDM has been commonly used in the past few decades in different studies and has been employed successfully in GWPZ mapping. However, despite the universality of AHP, it is often criticized owing to its manner of handling inherently ambiguous and imprecise mapping data. Moreover, the MCDM-AHP technique has been applied in arid as well as semi-arid regions for groundwater potential mapping in several areas of the world (Ajibade et al., 2019). However, in none of these techniques was Fuzzy set theory integrated into MCDM, as in Fuzzy-AHP. The integration of Fuzzy-AHP may lead to improvement in the accuracy of groundwater potential mapping, owing to the flexibility of the functions of Fuzzy membership. On this basis, the current study uses the combined RS-GIS method along with Fuzzy-AHP to develop thematic data layers to delineate GWPZ in Shanxi Province, China.

3.3.1. AHP model

The criteria weights were determined by employing pairwise ranking with the rank–sum method of AHP. AHP was originally developed by Saaty (1990) and is often known as the Saaty method (Coyle, 2004). It is an organized template and technique that assists the user with handling complicated decisions. It helps decision-makers to identify the best possible ways to understand the problems encountered. However, the strength of the model is evaluated by the consistency ratio (CR), which has three basic principles-decomposition, relative judgment, and priority synthesis. It is based on pairwise comparisons concerning the element at the next upper hierarchical level (i.e., among variables and indicators). The ratings of the features are denoted as numerical values with the comparison matrix. Based on this, the relative weights of all aspects can be calculated by the priority level in the hierarchy. The comparative importance of factors in the pairwise matrix was determined by applying the Saaty rating scale. A pairwise comparison approach was adopted to calculate the relative importance of the factor. Table 2 reveals the Saaty pairwise rating scale. Numeric values (1–9) are allocated on the basis of the significance of the factors (Coyle, 2004).

In this study, seven thematic maps and their respective features are given appropriate relative weights from 1 to 9 through the Saaty rating scale (Table 2). There is no typical method for the pairwise comparison; however, assuming that geomorphology is determined to be absolutely more significant, owing to its important effect on groundwater, the weight for geomorphology was assigned as 9. There were seven factors

Table 2
Weight assignment criteria for the thematic map.

No.	Theme	Assigned weight
1	Geomorphology	9
2	Soil	8
4	Rainfall	7
5	Slope	6
6	Drain density	5
3	LULC	3
7	NDVI	2

1-Equal Importance, 3-More important, 5-much more important, 7-very much more important, 9- absolutely more important, 2, 4, 6, 8- intermediate values. These values come from Saaty's pairwise rating scale

those influence GWPZ. First, it is important to provide an initial matrix for pairwise comparison between variables, as every variable is as important by itself. Then, it considered that rainfall to be a very much more important factor in terms of groundwater recharge then drain density. So, 7 was assigned rainfall and 5 for drain density. Due to LULC and NDVI has less influence on groundwater, the weights are defined as 3 and 2, respectively. Similarly, it was measured that geomorphology is absolutely more important to impact on groundwater. The value of 9 was assigned for geomorphology. For soil and slope 8 and 6 were assigned because they considered as intermediate values for GWPZ. This study similarly judges and provides values for the other factors based on the influence toward the groundwater potentiality. Table 2 shows the weight assignment criteria of other factors (thematic maps).

3.3.2. Fuzzy logic model

The Fuzzy model is proposed by Zadeh (1965). It is the modeling and simulation technique for complex systems. In spatial planning, it is generally used when decisions are made to execute the spatial objects of a map as the set members. However, with the Fuzzy set model, the membership value of a particular object denotes the level of membership function (Zadeh, 1965). The triangular Fuzzy number (TFN) $\tilde{M}$ is exhibited in Fig. 3.

The primary function of the Fuzzy model is to make the data ambiguous. Mathematics as well as programming functions are acceptable for application in the Fuzzy model. For GWPZ mapping, the Fuzzy

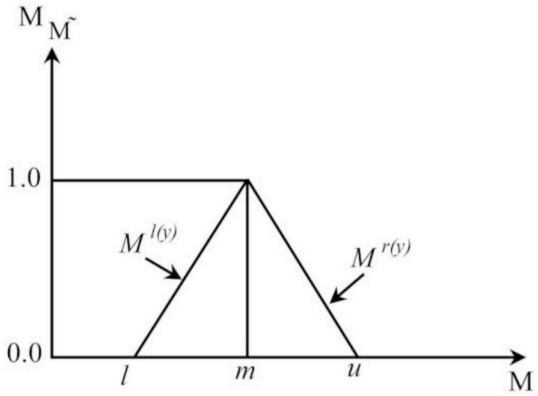

Fig. 3. A triangular Fuzzy number (TFN) M~.

Table 3
Five levels with Fuzzy numbers.

Levels	Fuzzy numbers
Very low	0, 0, 0, 3
Low	0, 3, 3, 5
Medium	3, 5, 5, 7
High	5, 7, 7, 10
Very High	7, 10, 10, 10

model permits the concept of incomplete location membership and considers the various groups. In this theoretical background, the Fuzzy membership function (FMF) is assigned to analyze the spatial variation and patterns that lead to the establishment of Fuzzy borders for all potential zones. In this study, FMFs for each possible zone are attributed to the variance as their trend evolved from Fuzzy boundaries, and five different factors were weighted, with each factor weight representing separate evaluations in Fuzzy language (Table 3). For instance, the medium-level is expressed as 3, 5, 5, and 7 in FMF.

3.3.3. wt assignments and normalization

The purpose of AHP is to account for expert knowledge; however, AHP cannot rely solely on human decisions. Therefore, the integration of Fuzzy analysis and AHP (Fuzzy-AHP) was established to solve Fuzzy hierarchical problems. In this study, the Fuzzy-AHP technique is applied to fuzzify the hierarchical analysis with Fuzzy numbers and is applied to pairwise comparisons to evaluate Fuzzy weights. To assess the weights of selected criteria by Fuzzy-AHP, the following steps were considered.

Stage I: Pairwise comparison matrix was developed employing all of the criteria in a hierarchical system. Philological principles were used for pairwise evaluations, and in all conditions, one of the two parameters were more relevant.

Judgment matrices (A) can be established by pairwise comparison by AHP as

$$A = \begin{bmatrix} A_{11} & A_{12} & \cdots & A_{1n} \\ A_{21} & A_{22} & \cdots & A_{2n} \\ \vdots & \vdots & \ddots & \vdots \\ A_{n1} & A_{n2} & \cdots & A_{nn} \end{bmatrix} = \begin{bmatrix} A_1/A_1 & A_1/A_2 & \cdots & A_1/A_n \\ A_2/A_1 & A_2/A_2 & \cdots & A_2/A_n \\ \vdots & \vdots & \ddots & \vdots \\ A_n/A_1 & A_n/A_2 & \cdots & A_n/A_n \end{bmatrix} \quad (1)$$

where A_n denotes the nth indicator element with A_{ij} as the judgment matrix element.

Traditional AHP performs a clear determination and is accompanied by uncertainty. Therefore, it is unable to reflect human thinking effectively. Fuzzy logic is an advanced logical method developed based on the conventional AHP process. In the normalization method, the matrix element is expressed by TFN. TFN can avoid ambiguity, inaccuracy, and uncertainty. To compare the results of the two techniques, weights were adopted using the same Saaty rating system. The numbers 1/2, 1, 3/2, 2, 5/2, 3, 7/2, 4, 9/2, and 5 were used for the Fuzzy scaling ratios, representing the strength of one component over the other with interim values, rather than crisp numbers.

$$A_{ij} = (l, m, u) = \left(l, \frac{A_i}{A_j}, u\right) \quad (2)$$

where l, m, u are the minimum potential value, moderate probable value, and maximum possible value, respectively. A_{ij} the decision matrix element in equation (1).

Step II: Calculation of normalized weight

$$W_n = \left(GM \Big/ \sum_{n=1}^{N_f} GM_n \right) \tag{3}$$

where GM is the geometric average of the ith line of the decision matrices, which is calculated as

$$GM = \sqrt[N_f]{A_{1n}A_{2n}\cdots A_{nN_f}} \tag{4}$$

The weight is normalized, and the subjective weight is eliminated by the feature vector method. In addition, the consistency of normalized values was tested by calculating the CR of the subject variables and their categories. The CR of a matrix demonstrates the level of consistency in comparison with a randomly created matrix. The consistency ratio of the matrix (Table 4) was 0.0077, which is considered as an acceptable consistency (Saaty, 1990).

Step III: The accuracy of pairwise comparisons was calculated through the consistency index (CI). However, the consistency of judgements was checked by calculating the CR. The CR controls the balance in which weights are assigned. Although the weights are allocated through field experience, they should neither be over-estimated nor under-estimated but rather be as exact as possible. The acceptable CR level is < 0.10. The equation for CR is

$$CR = \frac{\text{Consistency Index (CI)}}{\text{Random Index (RI)}} \tag{5}$$

The Consistency Index (CI) for a matrix is calculated by the following equation

$$CI = \frac{\lambda_{max} - n}{n-1} \tag{6}$$

where λ_{max} is the maximum value (weight) of OPM and n is the number of criteria. The random index (RI) table (Table 5), created by Coyle, indicates the sum of the RI value in which the upper row is on the order (value of n) of that of a random matrix and the lower row corresponds to the consistency index for random decisions.

3.3.4. Spatial model for delineation of GWPZ

The multi-factor decision-making structure is created by calculating the selected factors of GWPZs. The model produces a GWPZ map by combining consistent thematic layers with weighted overlaid GIS data. In the weighted overlap study, both raster and vector data were equally applied. All the factors were combined, assigning a weight based on the importance of each attribute in the accumulated results. In addition, a weighted linear combination (WLC) of factors was then employed to create the GWPZ map.

Finally, the GWPZ map was produced in the GIS platform with the WLC of the separate criteria layers. The methodology of GWPZ desalination and the integration of RS, GIS, and Fuzzy-AHP technique is shown in Fig. 4. It shows that the first step involved generating the thematic layers including geomorphology, slope, NDVI, drainage density, rainfall, LULC, and soil type. In second step, Fuzzy-AHP applied to assign weights of the factors. Afterword, the thematic layers were integrated with overlay method in GIS environment. Finally, the GWPZ map generated with validation and sensitivity analysis. A raster calculator in ArcGIS was applied to the overlaid thematic maps. The groundwater probability index was calculated as:

$$\text{GWPZ} = \sum_{i=1}^{n} \sum_{j=1}^{m} w_i * x_j \tag{7}$$

where GWPZ is the map of groundwater potential zone, w_i denotes the normalized weight of the i^{th} thematic variable (Table 6), x_j indicates the normalized weight of the jth class of the variable (Table 4), n reveals the total number of variables, and m is the total number of classes of a variable.

3.4. Sensitivity analysis

Through sensitivity analysis, the impact of input criteria on the model output efficiency was assessed, and the influence of the adaptation of parameters/factors was validated. The influence of the data on the weighted values as well as the weights allocated to each factor was validated with sensitivity analysis. Equation (8) was applied to measure the effectiveness of each weight

$$\text{Effective weight} = \frac{\text{Theme}_w \times \text{Theme}_s}{\text{GWPI}} \times 100 \tag{8}$$

where w is the weight and s is the scale value of the factors assigned to each grid. GWPI indicates the groundwater potential index, as computed from Equation (8).

4. Results and discussion

4.1. Development of thematic maps

In the current study, RS satellite data are used to produce seven thematic parameters (layers) that affect groundwater potentiality in Shanxi Province, China. The thematic maps from geo-environmental data were deriving from conventional data/maps and RS data and created in fixed spatial scaling of selected factors. Thus, it does not denote individual characteristics of inhabitants. The layers are geomorphology, slope, NDVI, drainage density, rainfall, LULC, and soil type. However, the thematic maps/layers used to classify GWPZ vary across the study area, and the selection of assigned weights of the features/classes of the maps/layers is arbitrary (Table 6). The classes along with their respective ratings and the normalized weights of every factor are displayed in Table 6.

4.1.1. Slope

Slope difference has a crucial function in the replenishment of groundwater and delineation of GWPZs. Sites with flatter or lower slopes are good indicators of groundwater potential zones, since they provide more excellent rates of water renewal compared with regions of higher slope (Mumtaz et al., 2019; Nayyer et al., 2019). Slope is a vital factor

Table 4
The Fuzzy-AHP Normalized pairwise comparison matrix for groundwater potential zones.

	Slope	Geomorphology	Rainfall	Drain density	LULC	Soil	NDVI	Normalized weights
Slope	1,1,1	1/2,6/9,1	2/3,6/7.5,1	1,6/5,3/2	3/2,6/3,1	2/3,6/8,1	5/2,6/2,7/2	0.142946
Geomorphology	1,9/6,2	1,1,1	1,9/7.5,3/2	3/2,9/5,2	5/2,9/3,7/2	1,9/8,3/2	4,9/2,5	0.224727
Rainfall	1,7.5/6,3/2	2/3,7.5/9,1	1,1,1	1,7.5/5,2	2,7.5/3,3	2/3,7.5/8,1	3,7.5/2,7/2	0.181448
Drain density	2/3,5/6,1	1/2,5/9,2/3	1/2,5/7.5,1	1,11	1,5/3,3/2	1/2,5/8,2/3	2,5/2,3	0.122007
LULC	1,3/6,2/3	2/7,3/9,2/5	1/3,3/7.5,1/2	2/3,3/5,1	1,1,1	1/3,3/8,2/5	1,3/2,2	0.078786
Soil	1,8/6,3/2	2/3,8/9,1,	1,8/7.5,3/2	3/2,8/5,2,	5/2,8/3,3	1,1,1	7/2,8/2,9/2	0.199266
NDVI	2/7,2/6,2/5	1/5,2/9,1/4	2/7,2/7.5,1/3	1/3,2/5,1/2	1/2,2/3,1	2/9,2/8,2/7	1,1,1	0.05082
CR = 0.0077								

Table 5
Random average consistency indexes for various *n*.

n	1	2	3	4	5	6	7	8	9	10	11	12	13	14	15
RI	0.00	0.00	0.58	0.90	1.12	1.24	1.32	1.41	1.45	1.49	1.51	1.84	1.56	1.57	1.59

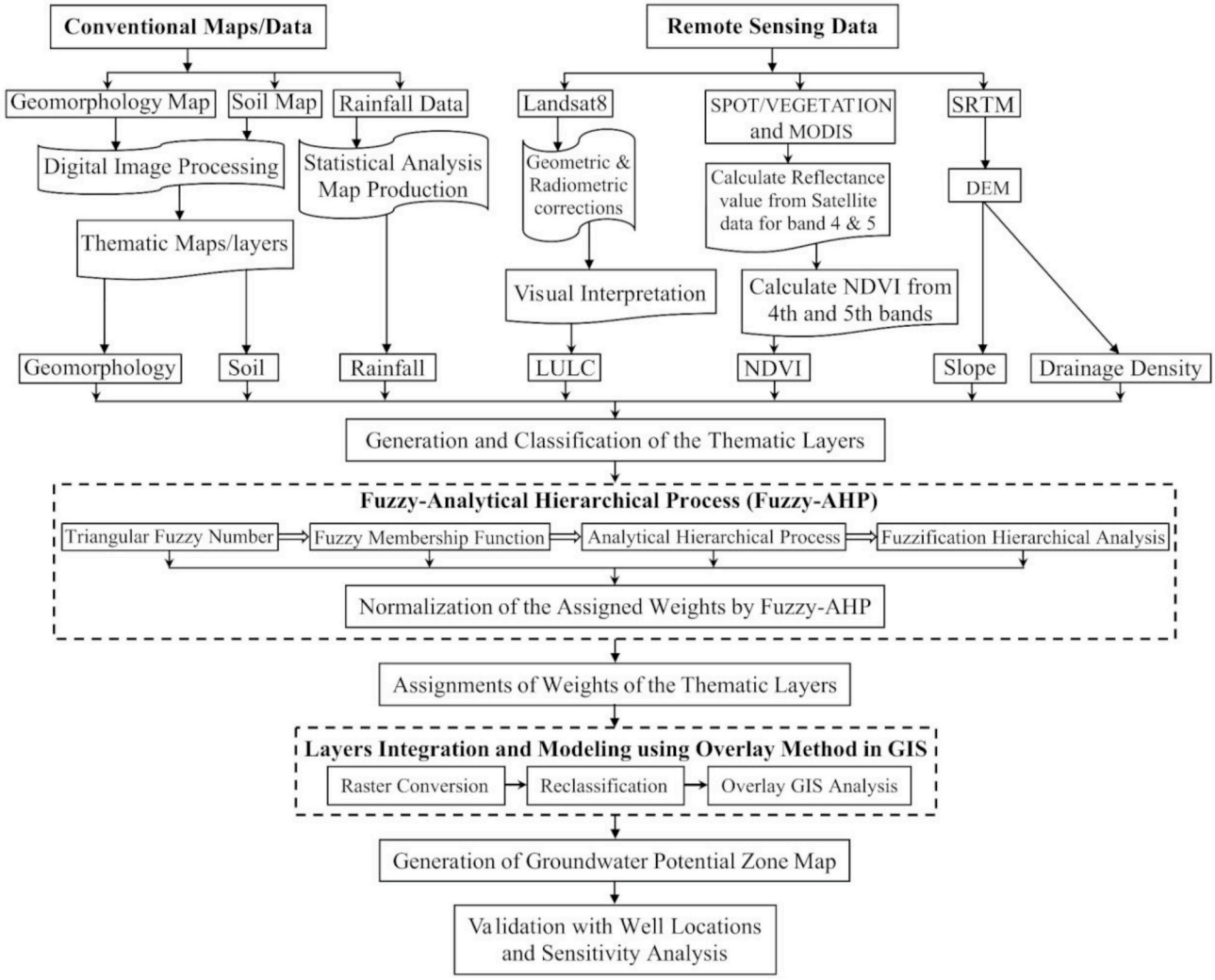

Fig. 4. Schematic flowchart of GWPZ mapping approach.

impacting the retention of water and amount of infiltrated precipitation. It is primarily responsible for erosion, surface runoff, and the transport of material. Water penetration capability is a property of slope, i.e., maximum penetration occurs when the slope is at a minimum, and the inverse is true as well (Patra et al., 2018; Sarker et al., 2020a). Highly elevated mountainous regions with elevated slope values are considered to exhibit a high flow of water with inadequate infiltration systems. In contrast, flat regions with low slopes can hold rainwater with increased high groundwater recharge capacity. However, to create a slope map, the most critical step is to develop the digital elevation model (DEM). A DEM with 500 m resolution is extracted from the SRTM data and is used to produce the slope map. The slope was derived from the DEM through the ArcGIS slope function. On the slope map, the slopes are classified into four broad groups (Fig. 5a). The elevation of the Shanxi Province ranges from 193 to 3004 m (Fig. 1). The sloping map varies from 0 to 41.86° and is divided into four categories: 0–0.03°, 0.03–0.07°, 0.077–0.13°, >0.1°, as seen in Fig. 5a. The category with the minimum slope is assigned the highest weight, owing to low runoff and extensive infiltration. In contrast, the class with maximum slope is given the lowest weight because of the likelihood of a poor groundwater supply (Agarwal and Garg, 2016). Consequently, areas with a lower degree of slope are considered suitable for groundwater potentiality, whereas areas with a higher degree of slope are considered as unsuitable for groundwater potentiality. Areas of 0–0.03° (approximately flat) fall into the excellent group, owing to flat topography, because the flat terrain shows a comparatively high penetration ratio and typically very good GWP region. Areas with slopes of 0.03–0.07° (gently sloping) are assumed to be worthy as a groundwater potential zone, owing to gently undulating topography and little surface runoff. Sites with a slope of 0.077–0.13° (steep-to-steep slope) correspond to relatively mild to minimum runoff and are, thus, classified as moderate GWP areas. Areas with slopes of >0.13° (very steep) are considered as having weak GWP zones, owing to the gradual and relatively high runoff and low infiltration rate.

Table 6
Assigned and normalized weights of the factors for seven thematic maps.

Thematic layers/ factors	Feature/Class	Area (%)	Assigned weight	Normalized weights
Slope	0–3	39.90	10	0.38
	3–7	36.94	8	0.31
	7–13	17.97	6	0.23
	13–41	05.18	2	0.08
Drainage density	0–0.032	33.46	10	0.38
	0.032–0.069	31.91	8	0.31
	0.069–0.111	24.19	6	0.23
	0.111–0.234	10.45	2	0.08
Soil	Sandy Loam	02.44	10	0.42
	Silty clay	47.63	8	0.33
	Silty clay loam	35.53	4	0.17
	Loam	14.41	2	0.08
Rainfall	>540 mm	08.77	8	0.40
	480–540 mm	18.20	6	0.30
	430–480 mm	51.07	4	0.20
	<430 mm	21.95	2	0.10
LULC	Water	1.002	10	0.31
	Cultivated land	38.25	8	0.25
	Bare land	0.094	6	0.19
	Grassland	29.15	4	0.13
	Forest	28.11	2	0.06
	Urban	03.38	2	0.06
NDVI	>0.8	26.07	8	0.32
	0.65–0.8	37.67	7	0.28
	0.50–0.65	24.83	6	0.24
	<0.50	11.43	4	0.16
Geomorphology	Platform	21.23	8	0.42
	Plain	20.17	6	0.32
	Mountain	37.00	4	0.21
	Hills	21.60	1	0.05

4.1.2. Geomorphology

Geomorphology has an important function concerning the presence of groundwater. The geomorphological map supports the classification of the form of geomorphic structures, different formations, and basal geology for providing an overview of the process, structures, materials, and geological controls of the groundwater context (Patra et al., 2018). It has a significant effect on the occurrence, storage, and recharging of water across the subsurface of the earth. Nevertheless, data from the "China Geomorphology Collection: 1:1 million" were used to generate the geomorphological map. Shanxi Province is dominated by plains, platforms, hills, and mountain ranges (Fig. 5b). The Plain is primarily in the shape of a basin in Shanxi. The province consists of the Plain (20.17%), plains (21.23%), hills (21.60%), and mountains (37.00%). Groundwater storage is believed to be very feasible in platforms, as most contain gentle hills, broad catchment areas, and water-resistant convex lenses. There is a substantial amount of good top-layer containing lagging water; hence, a high weight was allocated to platforms. Hills mostly consist of hard rock mass with a concentration of soil and a lack of necessary groundwater holes and caves; thus, low weight was assigned to hills. Groundwater in the mountain areas is also a source of interstitial water in the Tertiary loose coarse-grained rocks. In this case, the potentiality for groundwater availability is moderate-good.

4.1.3. Drainage network density

The density of the drainage system is directly related to the natural infiltration of the soil. It is also the most relevant parameter for hydrogeological study. The drainage system and density provide significant indication of the hydrogeological features of a region. It depends on the climate, penetration efficiency, lithology, vegetation intensity, relief, roughness, and drainage intensity index (Mahmoud and Alazba, 2016; Sarker et al., 2020c). Areas with high surface run-off demonstrate reduced groundwater potentiality owing to a low recharge ratio, caused by elevated drainage density. A drainage density map is extracted from DEM (Fig. 1), and the drainage intensity is produced applying the 'density analysis tool' of ArcGIS (Fig. 5c). The drainage density is defined by the closeness of the spacing between stream channels. The drainage density of a basin is the total length of the river network divided by the basin area, calculated by Equation (9).

$$D_N D = \sum \frac{L}{A} \tag{9}$$

where $D_N D$ is the density of the drainage network, L is the total length of the streams, and A denotes the area.

The drainage density varies from 0 to 0.234 km/km^2, and the drainage density is categorized into four classes: 0–0.032 km/km^2 (very good), 0.032–0.069 km/km^2 (good), 0.069–0.111 km/km^2 (moderate), and 0.111–0.234 km/km^2 (poor). It is inversely proportional to the terrain perviousness; therefore, areas with a low drainage intensity are strong indicators of water retention zones. High drainage intensity influences high runoff and indicates low groundwater likelihood. Higher weights are assigned to a poor drainage intensity region that develops a porous surface with greater infiltration and reduced surface runoff (Agarwal and Garg, 2016; Sarker et al., 2020b). Very good drainage intensity is identified in the middle part of Shanxi. Most of the study area is influenced by low drainage quality. Less porous rock results in less rainwater infiltration. A low drainage-intensity region provokes greater infiltration as well as reduced surface runoff relative to the high-drainage intensity area. This demonstrates that high-drainage density zones are not a fit for the GWP zones, owing to the high surface runoff (Achu et al., 2020; Adnan et al., 2020; Huq et al., 2020; Mohammadi-Behzad et al., 2018; Mumtaz et al., 2019; Yin et al., 2018).

4.1.4. Rainfall

The aquifers and groundwater are generally recharged by the effective rainfall. The level of rainfall is useful in assessing the volume of the groundwater reservoir, based on the ground properties (e.g., lithology, geology, and hydro-geomorphology). Elevated rainfall is related to strong groundwater potentiality (Chen, 2019; Minh et al., 2019). Rainfall is an essential part of the water cycle and a leading contributor to groundwater recharge. The rate and spatial-temporal distribution of rainwater have a significant impact on hydrology as well as hydrogeological conditions. Meanwhile, precipitation intensity and the combination of different favorable circumstances contribute to GWPZ detection. There is a strong possibility of additional groundwater in the event of high amounts of rain. In contrast, if the rainfall is low, then the groundwater potentiality is less. Rainfall differs not only temporally but also spatially. Therefore, it is essential for determining the impact of rainfall in identifying GWPZ. Geographic distribution of the mean annual precipitation map is developed by the Inverse Distance Weighting projection technique in the ArcGIS environment. Rainfall data were derived from the precipitation spatial interpolation data set of 108 national meteorological stations from the Shanxi Province. Shanxi is located in the tropical monsoon climate, and rain occurs mostly in the summer, attributable to oceanic influence. The total yearly rainfall in the Shanxi region is 380–645 mm, in which the eastern and southern parts of the province experience the greatest volume of rain. The precipitation map is divided into four classes: <430 mm (21.95%), 430–480 mm (51.07%), 480–540 mm (18.20%), and >540 mm (8.77%) (Fig. 5d). A class with a higher rainfall rate is assigned the highest weight, correlated to an increased groundwater recharge rate and high GWP, whereas a lower rainfall rate is assigned a smaller weight.

4.1.5. Soil type

The soil plays a notable role in the percolation and infiltration of surface water into the aquifers. Consequently, soil quality is crucial in the amount of recharge water infiltration into the subsurface (Ahmad

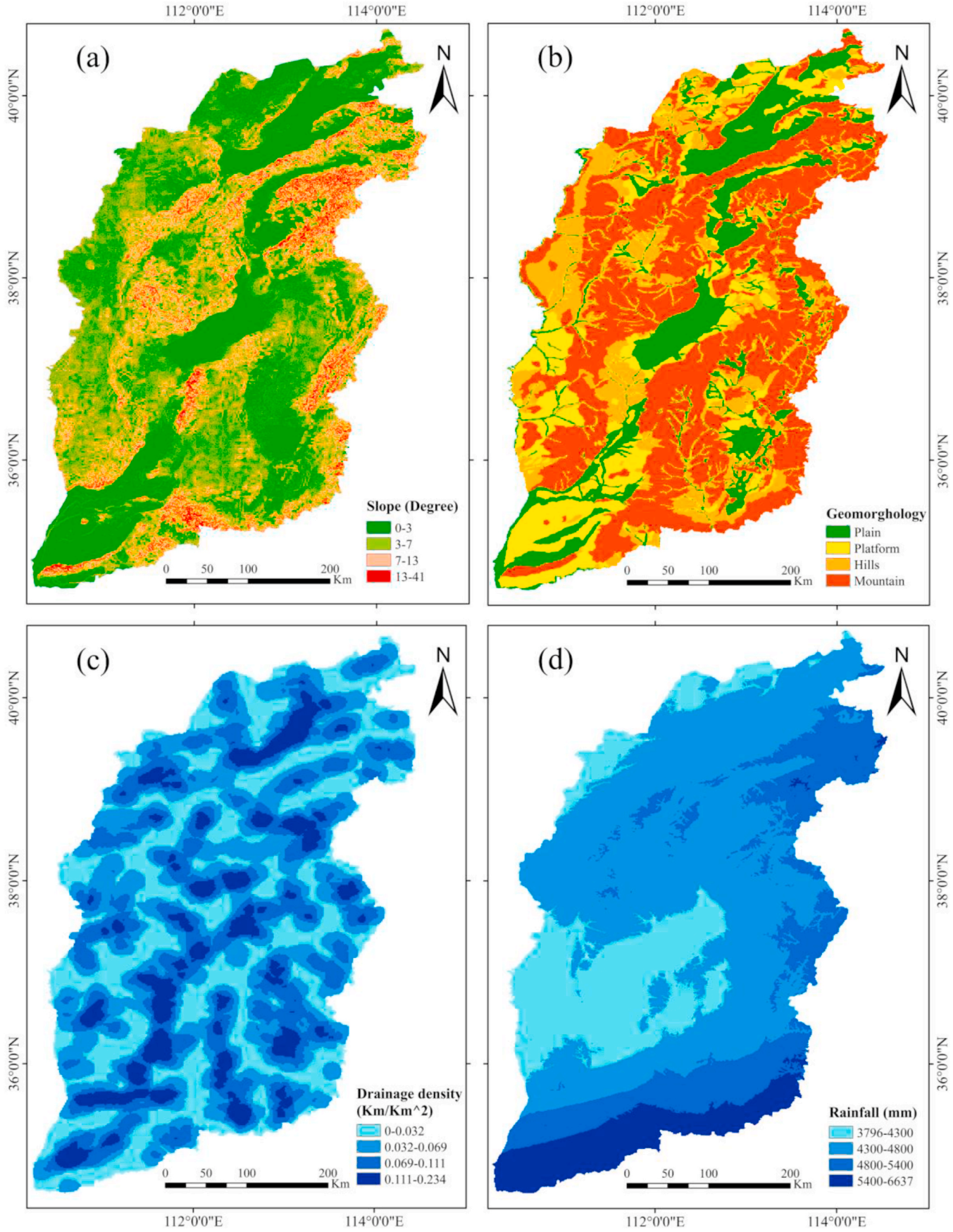

Fig. 5. (a) Slope (b) Geomorphological (c) Drainage density and (d) Rainfall map of the Shanxi Province, China.

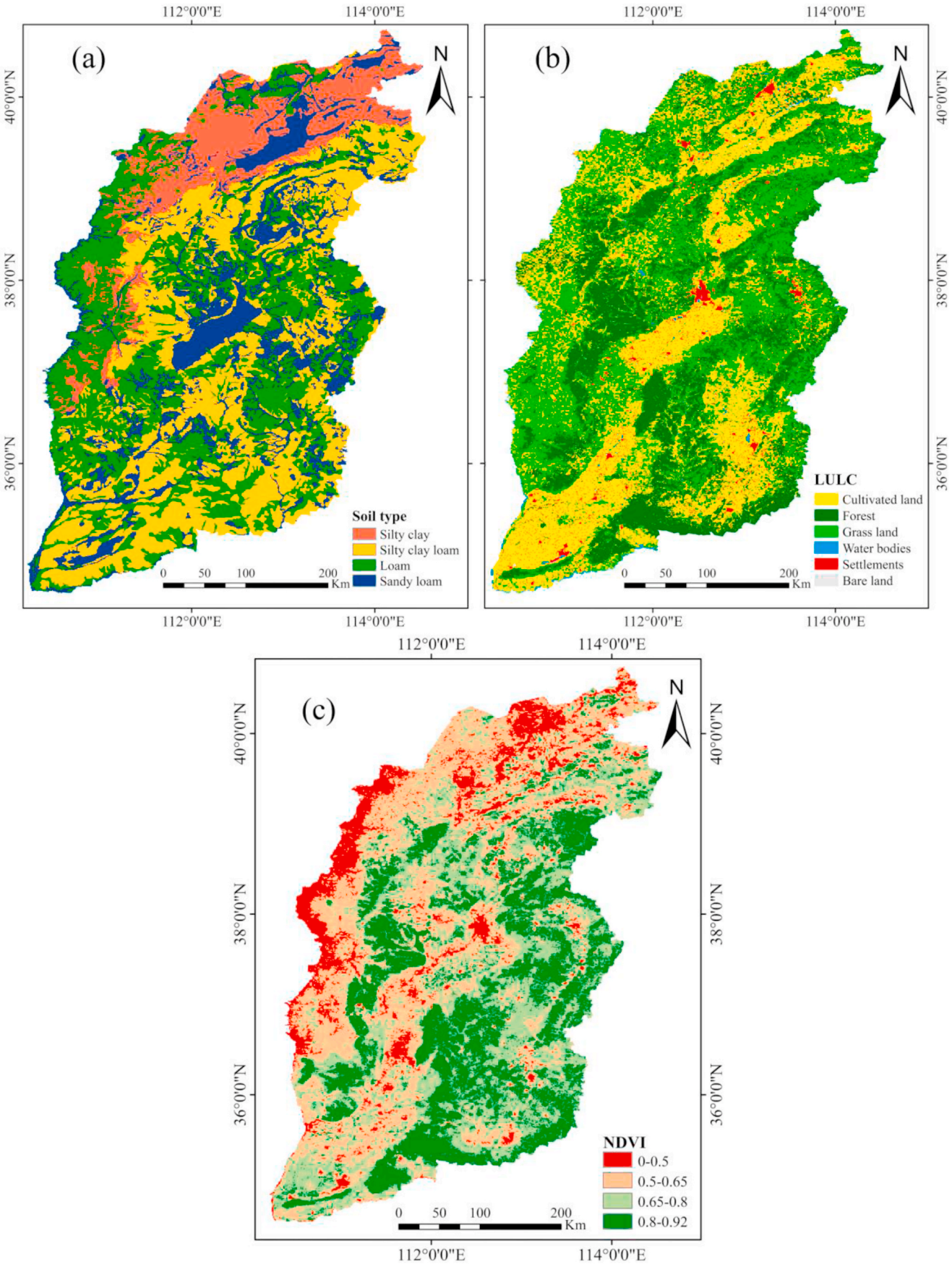

Fig. 6. (a) Soil type (b) Land use and land cover and (c) NDVI of study area.

et al., 2020). The infiltration and soil porosity of water primarily depend on the soil texture; then, the texture promotes the delineation of the GWPZ. Infiltration is mostly responsive to soil porosity and surface runoff. Less penetrable soil leads to surface runoff, enabling less infiltration, whereas porous soil contributes to increased water recharge (Siddi Raju et al., 2019). The soil map is created based on the data of 1:1 million soil maps of China. The study region is defined by four primary soil types (as seen in Fig. 6a), namely, silty clay (47.63%), silty clay loam (35.53%), loam (14.41%), and sandy loam (2.44%). Based on the soil condition and penetration rate, different weights were assigned to each soil unit. Sandy loam has a thicker soil base, lighter soil texture, and higher soil nutrient quality; meanwhile, it covers a small area, extremely suitable for groundwater storage. Consequently, it was assigned the maximum weight. Loam is commonly spread in various areas of the world, with a relatively scattered distribution. The transition border of other neighboring soil types is apparent, accounting for 47.63% of the Shanxi Province. Loam is found to be very good for groundwater storage and constitutes coarse particles, with less clay material, high water porosity, and drought susceptibility (Mumtaz et al., 2019). Silty clay loam is dissolved by seepage water and, afterwards, flows to the lower layer; thus, the organic matter quality of the leached soil is relatively high. Owing to its high content of clay, it is considered to be moderately suitable for groundwater storage. The soil type exhibiting the worst water permeability is silty clay, which is mainly distributed along the northwest of Shanxi Province.

4.1.6. Land use/land cover

LULC change has become one of the leading human-induced functions influencing the occurrence as well as recharge of groundwater resources. LULC has an important influence on the occurrence and renewal of groundwater in terrains. A specific factor, such as LULC, was then investigated to address human intervention with groundwater. Agricultural development can also enhance groundwater restoration (Chen et al., 2019; Mumtaz et al., 2019). Meanwhile, LULC changes could alter recharge rates, which could have negative implications for groundwater quality, particularly in arid and semi-arid areas such as Shanxi. They are a major factor influencing the recharging cycle of groundwater because of the impact on evapotranspiration, drainage, and recharging of the groundwater system. Fig. 6b displays the LULC map, which was prepared from the Landsat 8 remote sensing images. The LULC map is classified into six categories: forest (28.11884%), cultivated (38.25239%), grassland (29.15446%), water (1.00244%), barren land (0.09443%), and urban (3.377426%). Cultivated land constitutes the largest LULC, and the smallest LULC is occupied by barren land. Water bodies, cultivated, and barren fields are strong sources of groundwater storage, because agricultural land enables further water absorption, owing to the pore spaces in the soil. Meanwhile, the development of land decreases the penetration of water into the soil, owing to a lack of porous surfaces. Therefore, water penetration is decreased in the high impervious surface (urban areas); thus, the weight is lower for urban areas, since settlement areas are deemed as less important. However, the highest weight was assigned to water bodies, cultivated land, and bare land, whereas the lowest weights were assigned to grassland, urban areas, and forests, as defined in the GWPZ (Table 6).

Table 7
Statistical results of map sensitivity analysis.

Factors	Min	Max	Mean	SD
Slope	0.44	1.21	0.76	0.129
Geomorphology	0.37	1.18	0.69	0.121
Rainfall	0.42	1.18	0.72	0.127
Drainage density	0.44	1.25	0.77	0.124
LULC	0.45	1.30	0.81	0.129
Soil	0.43	1.09	0.67	0.093
NDVI	0.45	1.34	0.83	0.136

4.1.7. Normalized difference vegetation index

The NDVI is based on the proportion of photosynthetically absorbed radiation. An NDVI zero value denotes no green plants, and a value of approximately +1 (0.8–0.9) describes the maximum possible intensity of green vegetation. Fig. 6c shows the NDVI of the study area. NDVI is measured based on per-pixel and considers the standardized variation of red and near-infrared (NIR) bands of an image (Equation (10)).

$$NDVI = \frac{\text{NIR} - \text{RED}}{\text{NIR} + \text{RED}} \tag{10}$$

The biophysical analysis of NDVI is an element of consumed photosynthetically activated radiation. NDVI is an aspect that is an indirect factor of groundwater potentiality, since high vegetation cover is often demonstrated in areas in which shallow groundwater is available. Consequently, a higher weight is associated with a higher NDVI value (Table 7). The NDVI value in the Shanxi region is classified into four classes (<0.5, 0.5–0.65, 0.65–0.8, >0.8). These four groups cover 11.43%, 24.83%, 37.67%, and 26.07%, respectively, of the study area. The existence of underlying rock, elevation, and vegetation cover often affect penetration and surface runoff. Distinct or elevated bedrock optimizes runoff. In addition, areas of higher altitude and shallow vegetation cover or deforestation rapidly increases runoff.

4.2. Groundwater potential zoning

Van Laarhoven and Pedrycz introduced the concept of Fuzzy logic in AHP, utilizing the advantages of both Fuzzy and AHP techniques. Over the past few decades, Fuzzy-AHP has become the most commonly recognized multi-criteria decision-making approach for numerous types of study, such as groundwater quality evaluation (Minh et al., 2019), landslides (Mallick et al., 2018), ecosystem and environmental vulnerability (Li et al., 2009), groundwater susceptibility (Nadiri et al., 2017), and water quality extraction (Azimi et al., 2018). The capability of the proposed GIS-induced Fuzzy-AHP model of this study has also made its application more practical and useful. The spatial ranges of the GWP zones were defined based on the empirical consideration of seven thematic layers. In the model, various spatial investigation tools were applied to address spatial difficulties in the definition of possible groundwater potential zones. Potential groundwater areas for the study region, demarcated by the synthesis of several factors, including geomorphology, slope, rainfall, NDVI, drainage density, LULC, and soil type, were used with RS-GIS methods. The analytical results of this study highlight the weighted overlap analysis method employing GIS-based Fuzzy-AHP methodology, the most powerful technique for analyzing potential groundwater areas. The delineation of possible groundwater regions was performed in a group or cluster, and the interpreted layers were developed applying 'weighted overlay classification' with the spatial analyst method in ArcGIS.

In the province of Shanxi, China, conducting groundwater potential research is needed owing to the occurrence of industrial and agricultural development. The GWPZ map of Shanxi Province (Fig. 7) shows five separate groups (zones) illustrating very good, good, moderate, poor, and very poor groundwater probability zones in the region. Usually, very good and good GWPZ are associated with significant groundwater levels, which are calculated by different factors. Areas with flat, gentle hill, porous, and unconsolidated terrains are the most appropriate for groundwater conservation. The region covered by the very good GWPZ is roughly 207,784.2 km^2 (13.26%). The very good GWPZ of the study region covers the southwestern portion. The good GWPZ is distributed across the study area, representing 27.02% (423,403.4 km^2) of the total area. However, most of the good GWPZ is identified in the central and northern regions. The moderate GWPZ contains mostly concentrated scattered patches and is uniformly spread throughout the area. It occupies a region of 412,904.5 km^2, which is roughly 26.35% of the entire area, representing the largest GWPZ area among all classes. However, the western and middle parts of Shanxi fall under poor as well as very

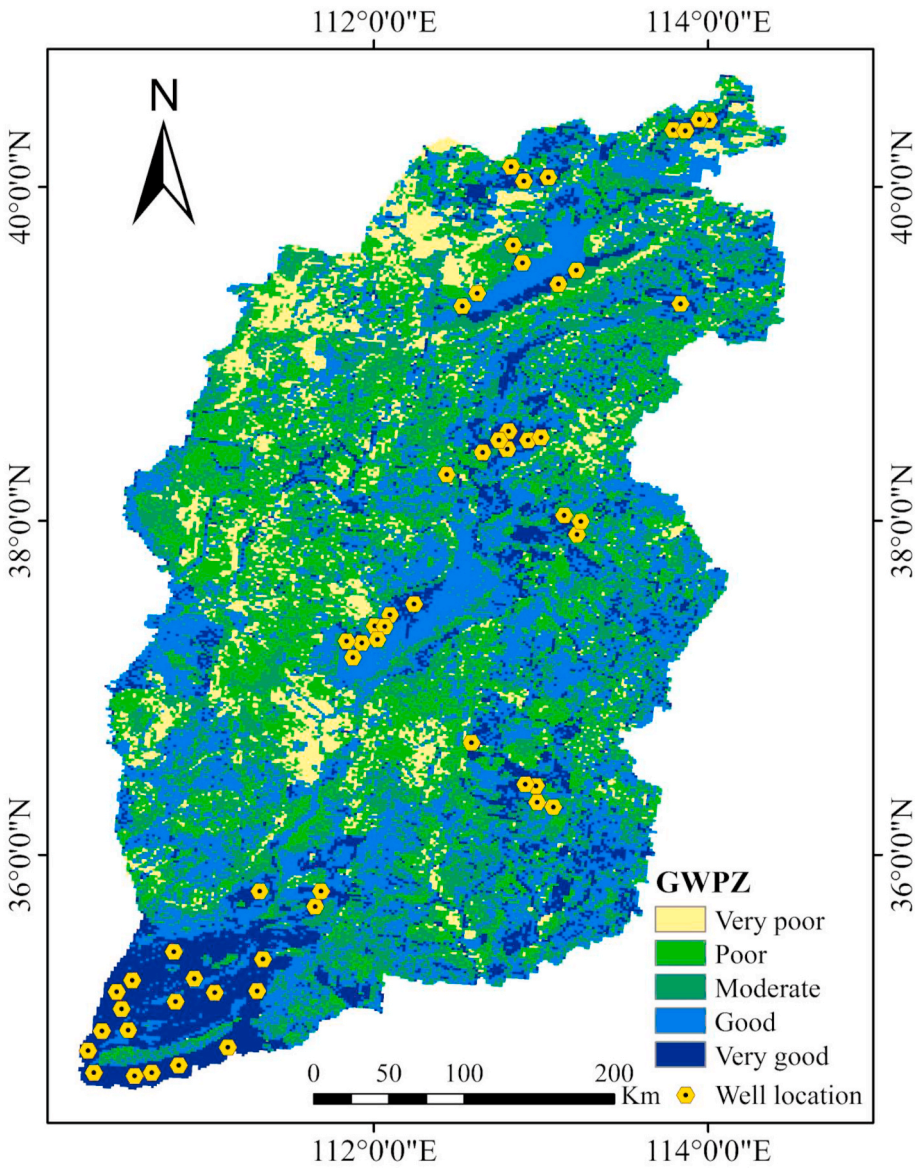

Fig. 7. Groundwater potential zones map of Shanxi Province, China and model validation through the wells.

poor GWPZ, occupying an area of approximately 370,438.8 km^2 (23.64%) and 152,155.7 km^2 (9.71%), respectively, because of its elevated slope with adverse geological (Pleistocene period deposition) as well as geomorphological (lateritic pediplain) conditions. This region is included under poor and very poor GWPZ. Usually, poor and very poor GWPZ have weak discharge ratios (volume/time) relative to good and moderate GWPZs.

The significance this study provides a comprehensive basis for planning sustainable groundwater strategies as well as management in Shanxi province. The findings show key implications to design sustainable groundwater strategy. As the methodology implemented in the study is emerged from reasonable conditions with generic nature. This general approach of GWPZ delineation is supposed for ensuring sustainable management of aquifer development. The GWPZ approach particularly underlines to promote groundwater conservation, application of appropriate scientific plan, regulating domestic as well as industrial water preservation practices leading to sustainable groundwater strategies. It may helpful for the long-term groundwater evolution practices in study area. Moreover, appropriate groundwater evolution plan implementation could lead for the better storage as well as groundwater management considering quality and quantity.

4.3. Model validation GWPZ maps

To verify the accuracy of the logic-based Fuzzy-AHP model, the findings derived from the proposed model are compared with 57 existing water well locations with the GWPZ map. Water well locations were obtained from the Distribution of Regional Groundwater Testing Stations (http://www.cigem.cgs.gov.cn/) of Shanxi Province, China, and the data from these locations were used in groundwater evolution study, strongly supporting geological hazard mitigation and the conservation of the geological environment. These locations offer appropriate facilities for critical national policy initiatives, such as natural resource management, the utilization and security of water supplies, and the development of sustainable civilizations. However, the deepest drilling depth was 291,509 m. The validation of the methodology relies on associating existing groundwater wells with the GWPZ map, applying proximity analytical tools in ArcGIS. The locations of the wells were also plotted on the subsequent GWPZ map using ArcGIS. The findings revealed that 82.5% (47 wells) and 12.3% (7 wells) of the total water wells are associated with very good and good GWP regions, respectively, whereas 3.5% (2 wells) belongs to moderate and 1.7% (1 well) corresponds to poor and very poor areas (Fig. 7). This suggests that the model-

generated GWPZs were consistent with ground-truth data, i.e., water-well data as well as most of the active wells are located in very good and good zones of the GWPZ map. This illustrates the ability of RS and GIS technologies to delineate GWPZs, which might help locate the appropriate locations to extract groundwater. These validation findings demonstrate that the database as well as methods applied to build GWPZ models for probable groundwater areas, through the analysis of the fitness of parameters and comparative significant weights of the factors, have produced accurate results.

4.4. Results of sensitivity analysis

Statistical analysis exhibited in Table 7 (derivative from Equation (8)) indicates a significant variance in the selected factors. This is mostly attributed to the existence of a floodplain as well as mature floodplain areas with the main river systems developed during Holocene period. This terrain (flat and gentle slope, porous, unconsolidated) is fit to store groundwater. This can demonstrate that farmland is perfect for groundwater recharge. NDVI impacts evapotranspiration, surface drainage, and groundwater renewal, which has an important effect on GWPZ detection. The GWPZ often tends to be sensitive to the impacts of geomorphology, slope, rainfall, drainage intensity, and soil quality. This may be due to the considerable statistical weights allocated to all the factors. Additionally, high average NDVI values, the drainage network, and slope indicate that the confining layers significantly influence the GWPZ. LULC, drainage rate, slope, geomorphology, soil composition, and precipitation all lead to differences in sensitivity. Their mean values are 0.81, 0.77, 0.76, 0.69, 0.67, and 0.72 respectively.

The GWPZ approach of this study could be applied for assessing potential groundwater zones in semi-arid region as well as other areas over the globe. For instance, if the purpose is to delineate GWPZ then on the basis of the geo-environmental situation of the given areas, a new GWPZ approach might be generated. Afterwards, the new GWPZ approach can be compared with the baseline of the proposed GWPZ approach. Moreover, contributing factors, variables, and indicators of the selection technique and weighing process can be modified to meet the requirements of a specified region.

5. Conclusions

Definitively, delineating the GWPZ using RS-GIS is difficult. However, a specific, scientific, and systematic method utilizing the Fuzzy-AHP model and RS-GIS technique have been successfully used to define and generate GWPZ maps in Shanxi Province, China, except the application of direct field data of groundwater reservation and flow. However, the findings of this study indicate that incorporating the Fuzzy-AHP model with the RS-GIS technique is a useful tool for groundwater potential zone mapping. This method offers accurate quantitative information of groundwater resources in a cost-effective manner, relative to traditional invasive methods. In this study, seven factors/thematic layers (geomorphology, slope, runoff, NDVI, drainage depth, LULC, and soil types) with various weights were incorporated into the model to produce the final GWPZ map. Each factor was categorized into several classes/features that closely regulate groundwater potentiality. The AHP and Fuzzy models were then applied to assign weights to each factor and standardize ratings. The GWPZ map was constructed by the normalized values with the Kriging feature interpolation method. The expected groundwater potential areas were classified into five groups, from very good to very poor. According to the GWPZ map of the entire province in this study, 207,784.2 km^2 (13.26%) was categorized as a very good groundwater potential area, 423,403.4 km^2 (27.02%) corresponded to good groundwater potential area, and the remaining 412,904.5 km^2 (26.35%), 370,438.8 km^2 (23.64%), and 152,155.7 km^2 (9.71%) were in the moderate, poor, and very poor categories. However, alluvial deposits have the highest potential for groundwater. Very good and good GWPZ strongly show that alluvial plains have excellent groundwater capacity. This study indicates that most of the parts of the province exhibit good to moderate potential for groundwater. The excellent groundwater possibility zone is situated in the southwest and central parts of Shanxi, resulting from the distribution of sedimentary plains and gentle slopes with high penetration capacity.

The findings of this study indicate that most of the areas with suitable gradients and rainfall patterns have high groundwater potentiality. Moreover, the GWPZ was compared with existing wells, and the Fuzzy-AHP model and the GIS-RS methodology was found to be basically in good agreement with the field data; thus, its validity was accepted. In addition, sensitivity analysis was conducted to better understand the function of each factor in depth. Sensitivity analysis revealed that NDVI and LULC had a noteworthy effect on the changes in GWPZ evaluation. The method introduced in this study should be verified by performing assessments of groundwater well discharge, depth data, and step-down drilling of wells at different locations in the watershed to determine the different groundwater-well yields in the different GWPZs. In this way, sustainable groundwater zones could be identified. However, the groundwater potential model is sensitive in assignment of weights of the factors/parameters and their associated classes/features, as the weight distribution method is somewhat arbitrary. Future research could examine the additional factors/variables that influence the identification of new GWPZs directly or indirectly. The GWPZ map provided by this approach can be used as an introductory guide for local authorities and water policymakers in the selection of appropriate drilling locations for new wells. The significance of this study is the establishment of a basic foundation to effectively formulate a plan for managing groundwater in Shanxi Province, China. The identification of zones where aquifers are formed may assist in balancing extraction as well as facilitating the sustainable development of groundwater supplies and provide scope for further research in groundwater extraction. The flexibility, logical conditions, and generic nature of the method can proceed with or without changes in the weights of the specified factors; therefore, this method can be implemented in different regions in China as well as all over the world.

Declaration of competing interest

The authors declare that they have no known competing financial interests or personal relationships that could have appeared to influence the work reported in this paper.

Acknowledgements

This study is supported with the National key R&D plan on strategic international scientific and technological innovation cooperation of special project under Grant 2016YFE0202300, the National Natural Science Foundation of China under Grants 41890820, 41771452 and 41771454, the Natural Science Fund of Hubei Province in China under Grant 2018CFA007, Natural Science Foundation of Inner Mongolia Autonomous Region (Project No.: 2019MS04017), Scientific research project of colleges and universities in Inner Mongolia Autonomous Region (Project No.: NJZY20277), and the State Key Laboratory of Information Engineering in Surveying, Mapping and Remote Sensing Special Research Funding.

References

Abijith, D., Saravanan, S., Singh, L., Jennifer, J.J., Saranya, T., Parthasarathy, K.S.S., 2020. GIS-based multi-criteria analysis for identification of potential groundwater recharge zones - a case study from Ponnaniyaru watershed, Tamil Nadu, India. HydroResearch 3, 1–14.

Achu, A.L., Thomas, J., Reghunath, R., 2020. Multi-criteria decision analysis for delineation of groundwater potential zones in a tropical river basin using remote sensing, GIS and analytical hierarchy process (AHP). Groundwater for Sustainable Development 10, 100365.

Adiat, K.A.N., Nawawi, M.N.M., Abdullah, K., 2012. Assessing the accuracy of GIS-based elementary multi criteria decision analysis as a spatial prediction tool – a case of

predicting potential zones of sustainable groundwater resources. J. Hydrol. 440–441, 75–89.
Adnan, K., Ying, L., Sarker, S., Yu, M., Eliw, M., Sultanuzzaman, M., Huq, M., 2020. Simultaneous adoption of risk management strategies to manage the catastrophic risk of maize farmers in Bangladesh. Geojournal.
Agarwal, R., Garg, P., 2016. Remote sensing and GIS based groundwater potential & recharge zones mapping using multi-criteria decision making technique. Water Resour. Manag. 30 (1), 243–260.
Ahmad, I., Dar, M.A., Teka, A.H., Teshome, M., Andualem, T.G., Tehsome, A., Shafi, T., 2020. GIS and fuzzy logic techniques-based demarcation of groundwater potential zones: a case study from Jemma River basin, Ethiopia. J. Afr. Earth Sci., 103860
Ajibade, F.O., Olajire, O.O., Ajibade, T.F., Nwogwu, N.A., Lasisi, K.H., Alo, A.B., Owolabi, T.A., Adewumi, J.R., 2019. Combining multicriteria decision analysis with GIS for suitably siting landfills in a Nigerian state. Environmental and Sustainability Indicators 3–4, 100010.
Arefin, R., 2020. Groundwater potential zone identification at Plio-Pleistocene elevated tract, Bangladesh: AHP-GIS and remote sensing approach. Groundwater for Sustainable Development 10, 100340.
Azimi, S., Moghaddam, M.A., Monfared, S.A.H., 2018. Spatial assessment of the potential of groundwater quality using fuzzy AHP in GIS. Arabian Journal of Geosciences 11 (7), 142.
Balezentiene, L., Streimikiene, D., Balezentis, T., 2013. Fuzzy decision support methodology for sustainable energy crop selection. Renew. Sustain. Energy Rev. 17, 83–93.
Cagman, N., Enginoglu, S., Citak, F., 2011. Fuzzy soft set theory and its applications. Iranian journal of fuzzy systems 8 (3), 137–147.
Carleer, A., Wolff, E., 2006. Region-based classification potential for land-cover classification with very high spatial resolution satellite data. In: Proceedings of the 1st International Conference on Object-Based Image Analysis. Citeseer, pp. 4–5.
Chen, G., 2019. Agricultural Water Efficiency Evaluation Method Based on Remote Sensing Technology, vol. 36. Revista de la Facultad de Agronomia de la Universidad del Zulia, 5.
Chen, G., Liu, X., Wang, Y., Tu, C., Kamruzzaman, M., 2019. Measurement of environmental pollution sources by electron microscope remote sensing image algorithms. Acta Microscopica 28 (5).
Chen, X.-l., Wei, J.-c., Guo, J.-b., 2010. Prediction on water abundance of sandstone by multiple factors analysis method. Shaanxi Coal 5.
Coyle, G., 2004. The Analytic Hierarchy Process (AHP). Practical Strategy: Structured Tools and Techniques.
Crétaux, J.-F., Calmant, S., Del Rio, R.A., Kouraev, A., Bergé-Nguyen, M., Maisongrande, P., 2011. Lakes Studies from Satellite Altimetry, Coastal Altimetry. Springer, pp. 509–533.
Gaber, A., Koch, M., El-Baz, F., 2010. Textural and compositional characterization of wadi feiran deposits, sinai peninsula, Egypt, using radarsat-1, PALSAR, SRTM and ETM+ data. Rem. Sens. 2 (1), 52–75.
Guo, H., Wang, Y., 2005. Geochemical characteristics of shallow groundwater in Datong basin, northwestern China. J. Geochem. Explor. 87 (3), 109–120.
Hall, D.K., Box, J.E., Casey, K.A., Hook, S.J., Shuman, C.A., Steffen, K., 2008. Comparison of satellite-derived and in-situ observations of ice and snow surface temperatures over Greenland. Remote Sens. Environ. 112 (10), 3739–3749.
Hu, S., Luo, T., Jing, C., 2013. Principal component analysis of fluoride geochemistry of groundwater in Shanxi and Inner Mongolia, China. J. Geochem. Explor. 135, 124–129.
Huq, M., Fahad, S., Shao, Z., Sarven, M.S., Imtiaz Ali, K., Mukhtar, A., Muhammad, S., Hidayat, U., Muahmmad, A., Shah, S., 2020. Arsenic in a groundwater environment in Bangladesh: occurrence and mobilization. J. Environ. Manag. 262.
Huq, M.E., Su, C., Fahad, S., Li, J., Sarven, M.S., Liu, R., 2018a. Distribution and hydrogeochemical behavior of arsenic enriched groundwater in the sedimentary aquifer comparison between Datong Basin (China) and Kushtia District (Bangladesh). Environ. Sci. Pollut. Control Ser. 25 (16), 15830–15843.
Huq, M.E., Su, C., Li, J., Sarven, M.S., 2018b. Arsenic enrichment and mobilization in the Holocene alluvial aquifers of Prayagpur of Southwestern Bangladesh. Int. Biodeterior. Biodegrad. 128, 186–194.
IPCC, 2001. Climate Change 2001: the Scientific Basis: Part of the Working Group I Contribution to the Third Assessment Report of the Intergovernmental Panel on Climate Change. IPCC.
Jasmin, I., Mallikarjuna, P., 2011. Satellite-based remote sensing and geographic information systems and their application in the assessment of groundwater potential, with particular reference to India. Hydrogeol. J. 19 (4), 729–740.
Lavender, S., Groom, S., 1999. Technical Note the SeaWiFS Automatic Data Processing System (SeaAPS).
Li, J., Han, L., Zhang, G., Su, Z., Zhao, Y., 2017. Temporal-spatial variations of human settlements in relation to environment change during the Longshan culture and Xia-Shang periods in Shanxi Province, China. Quat. Int. 436, 129–137.
Li, L., Shi, Z.-H., Yin, W., Zhu, D., Ng, S.L., Cai, C.-F., Lei, A.-L., 2009. A fuzzy analytic hierarchy process (FAHP) approach to eco-environmental vulnerability assessment for the Danjiangkou reservoir area, China. Ecol. Model. 220 (23), 3439–3447.
Liu, X., Pedrycz, W., 2009. Axiomatic Fuzzy Set Theory and its Applications. Springer.
M M, K., Saad Awadh, A., Madallah, A., Nasser, A., Muhammad Hameed, S., Enamul, MdH., 2020. Water resource evaluation and identifying groundwater potential zones in arid area using remote sensing and geographic information system. J. Comput. Sci. 16 (3), 266–279.
Ma, J., Li, D., Huq, M.E., Cheng, Q., 2020. Remote sensing detection and impact analysis of Tibetan human landscape in jiuzhaigou. The international archives of photogrammetry. Remote Sensing and Spatial Information Sciences 42, 629–633.
Mahmoud, S.H., Alazba, A., 2016. Integrated remote sensing and GIS-based approach for deciphering groundwater potential zones in the central region of Saudi Arabia. Environmental Earth Sciences 75 (4), 344.
Mallick, J., Singh, R.K., AlAwadh, M.A., Islam, S., Khan, R.A., Qureshi, M.N., 2018. GIS-based landslide susceptibility evaluation using fuzzy-AHP multi-criteria decision-making techniques in the Abha Watershed, Saudi Arabia. Environmental Earth Sciences 77 (7), 276.
Minh, H.V.T., Avtar, R., Kumar, P., Tran, D.Q., Ty, T.V., Behera, H.C., Kurasaki, M., 2019. Groundwater quality assessment using fuzzy-AHP in an giang province of vietnam. Geosciences 9 (8), 330.
Mohammadi-Behzad, H.R., Charchi, A., Kalantari, N., Nejad, A.M., Vardanjani, H.K., 2018. Delineation of groundwater potential zones using remote sensing (RS), geographical information system (GIS) and analytic hierarchy process (AHP) techniques: a case study in the Leylia–Keynow watershed, southwest of Iran. Carbonates Evaporites.
Mumtaz, R., Baig, S., Kazmi, S.S.A., Ahmad, F., Fatima, I., Ghauri, B., 2019. Delineation of groundwater prospective resources by exploiting geo-spatial decision-making techniques for the Kingdom of Saudi Arabia. Neural Comput. Appl. 31 (9), 5379–5399.
Murthy, K., Mamo, A.G., 2009. Multi-criteria decision evaluation in groundwater zones identification in Moyale-Teltele subbasin, South Ethiopia. Int. J. Rem. Sens. 30 (11), 2729–2740.
Nadiri, A.A., Gharekhani, M., Khatibi, R., Moghaddam, A.A., 2017. Assessment of groundwater vulnerability using supervised committee to combine fuzzy logic models. Environ. Sci. Pollut. Control Ser. 24 (9), 8562–8577.
Nayyer, S., Huq, M., Nana Yaw Danquah, T., Akib, J., Asif, S., 2019. Parameters derived from and/or used with digital elevation models (DEMs) for landslide susceptibility mapping and landslide risk assessment: a review. ISPRS Int. J. Geo-Inf. 8 (12).
Nhamo, L., Ebrahim, G.Y., Mabhaudhi, T., Mpandeli, S., Magombeyi, M., Chitakira, M., Magidi, J., Sibanda, M., 2020. An assessment of groundwater use in irrigated agriculture using multi-spectral remote sensing. Parts A/B/C 115 102810 Physics and Chemistry of the Earth.
Oikonomidis, D., Dimogianni, S., Kazakis, N., Voudouris, K., 2015. A GIS/Remote Sensing-based methodology for groundwater potentiality assessment in Tirnavos area, Greece. J. Hydrol. 525, 197–208.
Patra, S., Mishra, P., Mahapatra, S.C., 2018. Delineation of groundwater potential zone for sustainable development: a case study from Ganga Alluvial Plain covering Hooghly district of India using remote sensing, geographic information system and analytic hierarchy process. J. Clean. Prod. 172, 2485–2502.
Pinto, D., Shrestha, S., Babel, M.S., Ninsawat, S., 2017. Delineation of groundwater potential zones in the Comoro watershed, Timor Leste using GIS, remote sensing and analytic hierarchy process (AHP) technique. Applied Water Science 7 (1), 503–519.
Saaty, T.L., 1990. How to make a decision: the analytic hierarchy process. Eur. J. Oper. Res. 48 (1), 9–26.
Sarker, M.N.I., Wu, M., Alam, G.M.M., Shouse, R.C., 2020a. Life in riverine islands in Bangladesh: local adaptation strategies of climate vulnerable riverine island dwellers for livelihood resilience. Land Use Pol. 94, 104574.
Sarker, M.N.I., Wu, M., Alam, G.M.M., Shouse, R.C., 2020b. Livelihood diversification in rural Bangladesh: patterns and determinants in disaster prone riverine islands. Land Use Pol. 96, 104720.
Sarker, M.N.I., Yang, B., Lv, Y., Huq, M.E., Kamruzzaman, M., 2020c. Climate change adaptation and resilience through big data. Int. J. Adv. Comput. Sci. Appl. 11 (3), 533–539.
Shao, Z., Cai, J., 2018. Remote sensing image fusion with deep convolutional neural network. IEEE Journal of Selected Topics in Applied Earth Observations and Remote Sensing 11 (5), 1656–1669.
Shao, Z., Fu, H., Li, D., Altan, O., Cheng, T., 2019a. Remote sensing monitoring of multi-scale watersheds impermeability for urban hydrological evaluation. Remote Sens. Environ. 232, 111338.
Shao, Z., Wang, L., Wang, Z., Deng, J., 2019b. Remote sensing image super-resolution using sparse representation and coupled sparse autoencoder. IEEE Journal of Selected Topics in Applied Earth Observations and Remote Sensing 12 (8), 2663–2674.
Shao, Z., Yang, K., Zhou, W., 2018. Performance evaluation of single-label and multi-label remote sensing image retrieval using a dense labeling dataset. Rem. Sens. 10 (6), 964.
Siddi Raju, R., Sudarsana Raju, G., Rajasekhar, M., 2019. Identification of groundwater potential zones in Mandavi River basin, Andhra Pradesh, India using remote sensing, GIS and MIF techniques. HydroResearch 2, 1–11.
Silwal, C.B., Pathak, D., 2018. Review on practices and state of the art methods on delineation of ground water potential using GIS and remote sensing. Bull. Dep. Geol. 7–20.
Singaraja, C., Chidambaram, S., Anandhan, P., Prasanna, M.V., Thivya, C., Thilagavathi, R., 2015. A study on the status of saltwater intrusion in the coastal hard rock aquifer of South India. Environ. Dev. Sustain. 17 (3), 443–475.
Singh, L.K., Jha, M.K., Chowdary, V.M., 2017. Multi-criteria analysis and GIS modeling for identifying prospective water harvesting and artificial recharge sites for sustainable water supply. J. Clean. Prod. 142, 1436–1456.
Song, B., Park, K., 2014. Validation of ASTER surface temperature data with in situ measurements to evaluate heat islands in complex urban areas. Advances in Meteorology, 2014.
Steele, K., Carmel, Y., Cross, J., Wilcox, C., 2009. Uses and misuses of multicriteria decision analysis (MCDA) in environmental decision making. Risk Anal.: Int. J. 29 (1), 26–33.

Su, C., Zhu, Y., Abbas, Z., Huq, M.E., 2016. Sources and controls for elevated arsenic concentrations in groundwater of Datong Basin, Northern China. Environmental Earth Sciences 75 (7), 570.
Tang, Q., Xu, Q., Zhang, F., Huang, Y., Liu, J., Wang, X., Yang, Y., Liu, X., 2013. Geochemistry of iodine-rich groundwater in the taiyuan basin of central Shanxi province, north China. J. Geochem. Explor. 135, 117–123.
Todd, D.K., Mays, L., 1980. Groundwater Hydrology. John Willey & Sons. Inc., New York, p. 535.
Toth, J., 1963. A theoretical analysis of groundwater flow in small drainage basins. J. Geophys. Res. 68 (16), 4795–4812.
Turk, F.J., Miller, S.D., 2005. Toward improved characterization of remotely sensed precipitation regimes with MODIS/AMSR-E blended data techniques. IEEE Trans. Geosci. Rem. Sens. 43 (5), 1059–1069.
Xin-feng, L., Jiu-chuan, W., Yan-gang, S., 2012. Single factor Analysis on sandstone aquifer's water abundance in the coal seam's roof. Shandong Coal Science and Technology 5.
Yin, H., Shi, Y., Niu, H., Xie, D., Wei, J., Lefticariu, L., Xu, S., 2018. A GIS-based model of potential groundwater yield zonation for a sandstone aquifer in the Juye Coalfield, Shangdong, China. J. Hydrol. 557, 434–447.
Yousif, M., Sabet, H.S., Ghoubachi, S.Y., Aziz, A., 2018. Utilizing the geological data and remote sensing applications for investigation of groundwater occurrences, West El Minia, Western Desert of Egypt. NRIAG Journal of Astronomy and Geophysics 7 (2), 318–333.
Zadeh, L.A., 1965. Fuzzy sets. Inf. Control 8 (3), 338–353.
Zhang, K., Xie, X., Zhu, B., Meng, S., Yao, Y., 2019. Unexpected groundwater recovery with decreasing agricultural irrigation in the Yellow River Basin. Agric. Water Manag. 213, 858–867.
Zhang, Q., Rodríguez-Lado, L., Johnson, C.A., Xue, H., Shi, J., Zheng, Q., Sun, G., 2012. Predicting the risk of arsenic contaminated groundwater in Shanxi Province, Northern China. Environ. Pollut. 165, 118–123.
Zhang, Q., Rodriguez-Lado, L., Liu, J., Johnson, C.A., Zheng, Q., Sun, G., 2013. Coupling predicted model of arsenic in groundwater with endemic arsenism occurrence in Shanxi Province, Northern China. J. Hazard Mater. 262, 1147–1153.
Zhu, Y., Zhao, Y., Li, H., Wang, L., Li, L., Jiang, S., 2017. Quantitative analysis of the water-energy-climate nexus in Shanxi Province, China. Energy Procedia 142, 2341–2347.